Noise reduction in photorefractive image amplifiers and applications

J.-P. Huignard, H. Rajbenbach

▶ **To cite this version:**

J.-P. Huignard, H. Rajbenbach. Noise reduction in photorefractive image amplifiers and applications. Journal de Physique III, 1993, 3 (7), pp.1357-1367. 10.1051/jp3:1993204 . jpa-00249004

HAL Id: jpa-00249004
https://hal.science/jpa-00249004

Submitted on 4 Feb 2008

HAL is a multi-disciplinary open access archive for the deposit and dissemination of scientific research documents, whether they are published or not. The documents may come from teaching and research institutions in France or abroad, or from public or private research centers.

L'archive ouverte pluridisciplinaire **HAL**, est destinée au dépôt et à la diffusion de documents scientifiques de niveau recherche, publiés ou non, émanant des établissements d'enseignement et de recherche français ou étrangers, des laboratoires publics ou privés.

Classification
Physics Abstracts
42.65

Noise reduction in photorefractive image amplifiers and applications

J.-P. Huignard and H. Rajbenbach

Thomson-CSF, Laboratoire Central de Recherches, Domaine de Corbeville, 91404 Orsay Cedex, France

(*Received 20 February 1993, accepted 2 April 1993*)

Abstract. — We propose and experimentally demonstrate two original methods for suppressing the beam fanning noise of photorefractive amplifiers. The first one involves two wave mixing in a slowly rotating crystal, while the second requires to tilt the crystal with respect to the recording beams. This method applies to materials which exhibit a sharp resonance of the gain *versus* the pump-probe beam angle. With both methods a large improvement of the *S/N* ratio is achieved and virtually noise free image amplifiers are demonstrated. In $Bi_{12}SiO_{20}$, subpicowatt optical signals are detected and amplified. By using combinations of $LiNbO_3/Bi_{12}SiO_{20}$, as storage and amplification crystals respectively a long term readout (more than 20 hours) of a photorefractive memory is achieved.

1. Introduction.

It was early recognized that the photoinduced charge in electro-optic crystal (the photorefractive effect) provides unique opportunities for implementing highly non linear functions by mean of low power CW lasers. A wide variety of laboratory experiments have already been performed such as image amplification, pattern recognition, optical phase conjugation, associative memories and very promising capabilities exist for device applications in optical information processing or laser beam control. Current photorefractive crystals are the oxydes such as $LiNbO_3$, $BaTiO_3$, Bi_{12} (Si, Ge, Ti)O_{20} for the visible and semiconductors GaAs, InP, or CdTe for the near infrared spectral region. It is now recognized from experiments pursued with these crystals that large two wave mixing gain coefficient Γ can be achieved ($\Gamma \geqslant 5\text{-}10\ cm^{-1}$) for different operating conditions [1-4] (Applied DC or AC electric field, moving fringes, ..). In such conditions, when a weak optical signal is injected into a nonlinear photorefractive medium illuminated with a strong pump beam, it experiences gain through a two-wave process. A problem common to these amplifiers is the presence of noise sources that corrupt the quality of the emerging amplified optical signal. This problem is particularly disturbing for low-intensity injected signals and contributes to poor signal-to-noise ratios in the detection plane. In photorefractive amplifiers the spontaneous optical noise emission and

amplification (also called beam fanning) originates from light scattered in or reflected from the crystal imperfections and interfaces [2, 5]. A portion of this light propagates in the same direction as the injected signal and is also amplified through the formation of parasite noise gratings with the pump beam. Furthermore, the maxima of noise power obviously occur along the directions of maximum gain, i.e., in the directions that lie within the angular bandwidth of the photorefractive amplifier. Thus, it appears difficult to suppress the noise of photorefractive amplifiers efficiently while maintaining high gain for the signal. In this paper we will review and demonstrate two original methods which very significantly reduce the optical noise of the photorefractive amplifier while maintaining their high gain coefficient Γ. The first is based on a temporal filtering of the beam fanning, while the second takes advantage of the narrow angular bandpass of the photorefractive amplifiers like BSO or GaAs.

2. Noise reduction by crystal rotation.

This proposed method benefits form the slow build-up time constant of the noise gratings relative to the injected signal grating [6]. We will explain in the following that performing two-wave mixing (2 WM) in a slowly rotating crystal at angular velocity Ω results in a nearly complete washout of the noise gratings. The principle of operation is explained in the figure 1.

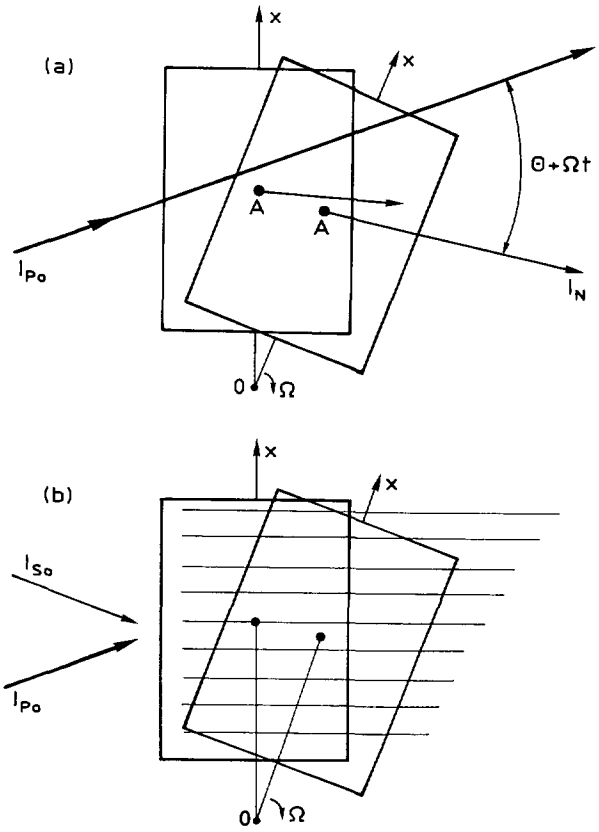

Fig. 1. — Schematic of the effect a crystal angular rotation (Ω) on (a) a noise grating, where $\theta + \Omega t$ is the time varying angle between the fixed pump beam and an internally generated noise beam originated from point A, and (b) the injected signal grating for which the rotation of the crystal yields a tilt of the illumination fringes. (The figures are not to scale.)

A noise source located near point A radiates a complex wave front whose component along the direction of the injected signal is represented by a plane wave of intensity I_N (A is a crystal imperfection or interface). It is essential to note that the noise sources are bounded to the crystal and consequently will move with it. This is the basis for the process of discrimination between the noise gratings and the injected signal grating. In the Ox coordinate bounded to the rotating crystal, the interference pattern responsible for the formation of a noise grating around point A is given by $I_N(x, t) = I_0[1 + m_N \cos K_N(t)\, x]$, where $K_N(t) \sim 2\pi(\theta + \Omega t)/\lambda$ is the modulus of the time dependent grating vector, and I_{P_0} is the pump intensity ; $I_{P_0} \gg I_S$. I_S is the signal beam intensity — $K_0 = 2\pi/\Lambda_0$ is the grating vector due to the coherent interference of the pump and signal beams. As an example, the noise distribution in the output plane of a photorefractive $BaTiO_3$ and BSO amplifiers is shown in the figure 2. These pictures reveal the angular dependence of the gain in a two dimensional mapping representation — large gain coefficients Γ are guaranted when injecting the signal beam I_s in the corresponding direction. The three principles involved will derive from the following remarks :

i) according to the above relation, a rotation of the crystal at angular velocity Ω may washout the noisy gratings ;

ii) during the crystal rotation, the injected grating K_0 is only slightly tilted and the grating period Λ_0 is not affected ;

iii) the build-up time of the noise gratings is always much longer than the build-up of the signal grating as shown in the figure 2.

From these considerations we can expect very different behaviors for the noise and the injected gratings *versus* the angular velocity Ω. This is clearly shown in the figure 3 which

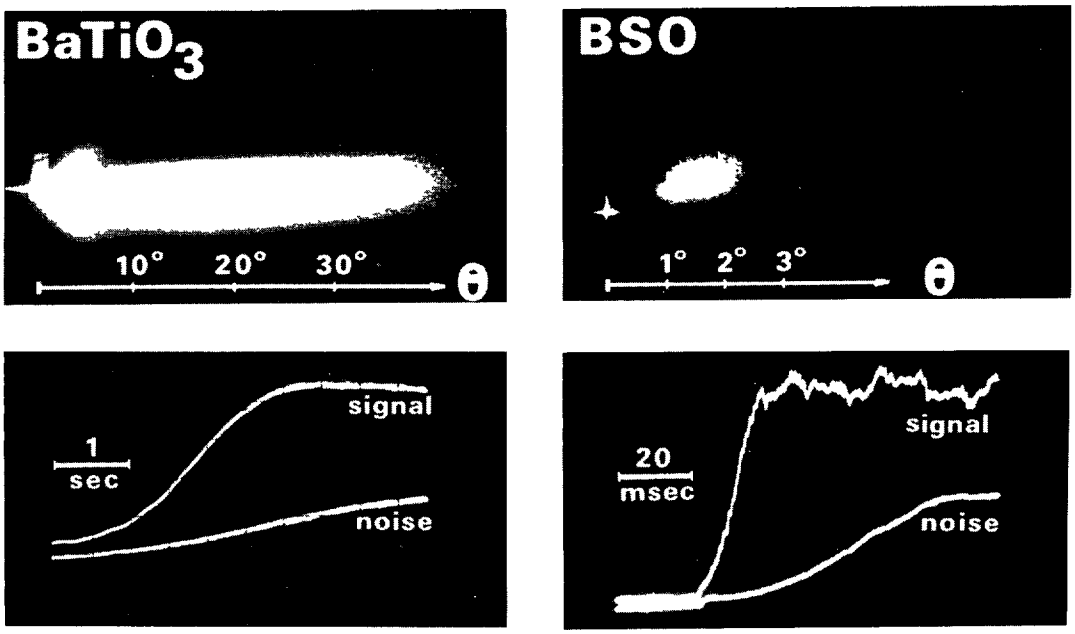

Fig. 2. — Top : the noise distribution in the output plane of photorefractive amplifiers ($\lambda_0 = 514$ nm, $I_{P_0} = 5$ mW/cm^2, $\Omega = 0$). The bright spots are the impact of the transmitted pump beams. Bottom : the time evolution of the noise and amplified signal emerging from photorefractive amplifiers when the pump beam is switched on. $\Lambda_0 = 2.5$ μm and $E_0 = 0$ for $BaTiO_3$, and $\Lambda_0 = 20$ μm and $E_0 = 8$ kV.cm^{-1} for BSO.

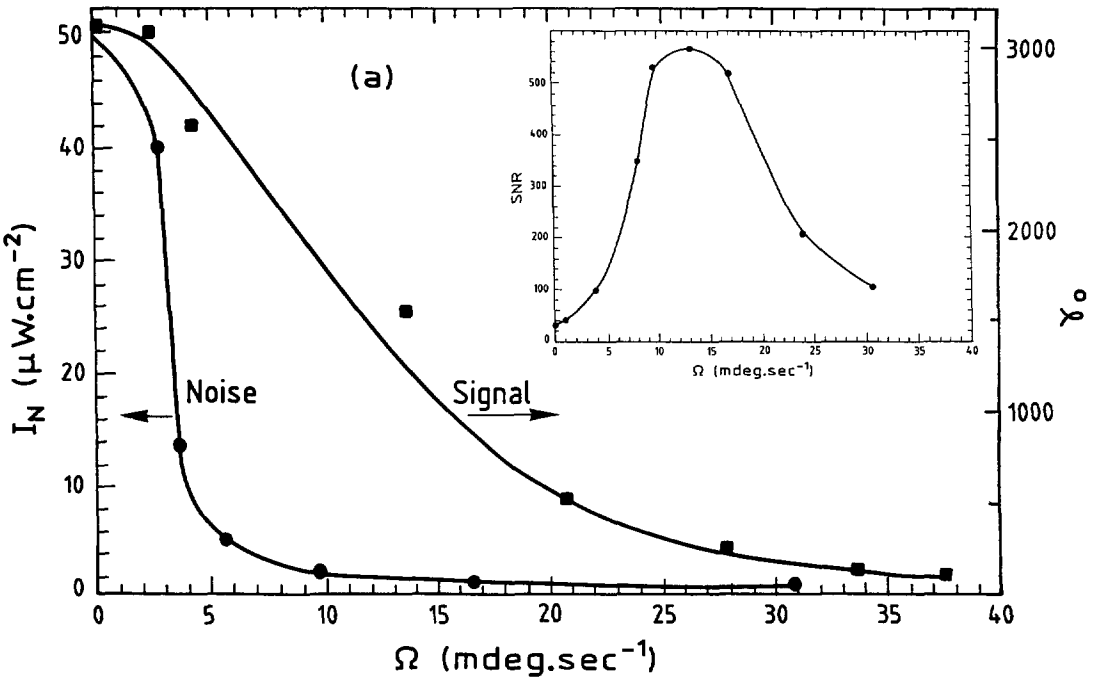

Fig. 3. — Noise power and two-wave mixing gain in $BaTiO_3$ *versus* the angular velocity of the crystal. The inset shows the dependence of the signal-to-noise ratio (SNR) on the angular velocity of the crystal.

outlines the fact that there exists an optimum angular velocity Ω_{opt} such as almost the noise gratings and fanning are eliminated while only a two fold reduction on the amplified signal intensity is observed [7]. For the involved operating conditions of $BaTiO_3$ — $I_{P_0} = 5\ mW.cm^{-2}$, $I_s = 5\ \mu W.cm^{-2}$, $\Lambda_0 = 2.5\ \mu m$ — this corresponds to a crystal velocity $\Omega_{opt} = 10\text{-}15\ m\ deg.s^{-1}$ for a large improvement of the signal to noise ratio (inset in Fig. 3) — γ_0 is defined as the intensity ratio I_s (with the pump)/I_s (with no pump) ; $\gamma_0 = \exp \Gamma\ell$ where ℓ is the crystal interaction length.

Similar experiments are performed in BSO crystals for the optimum fringe spacing $\Lambda_0 = 20\ \mu m$ using the drift mode ($E_0 = 8\ kV.cm^{-1}$) in a nearly degenerate 2 WM configuration. The experimental results in BSO are similar to those of $BaTiO_3$. The best SNR is obtained for $\Omega_{opt} = 1\text{-}2\ deg.s^{-1}$ and to maintain stationary gains over a large period, the crystal is placed on an electrically controlled rotation stage driven by a sawtooth voltage. Thus the crystal rotates at the optimum velocity and periodically quickly (i.e., faster than the response time τ_z) returns to its original position with its input face perpendicular to the incident beams. Gains of $\gamma_0 \sim 50$ and a signal-to-noise ratio improvement of a factor of ~ 5 are experimentally obtained in a 1 cm-thick BSO crystal.

To demonstrate noise-reduced image amplification, photographic transparencies are inserted across the signal beam path (Fig. 4). For $\Omega = 0$, the amplified images ($\times 10^3$ and $\times 50$ for $BaTiO_3$ and BSO, respectively) are corrupted by a strong background amplified scattered noise and multiple-interface-reflection parasite images for $BaTiO_3$. In the amplified images, using the rotating crystal technique all the noise has been removed and the parasite amplified images have disappeared.

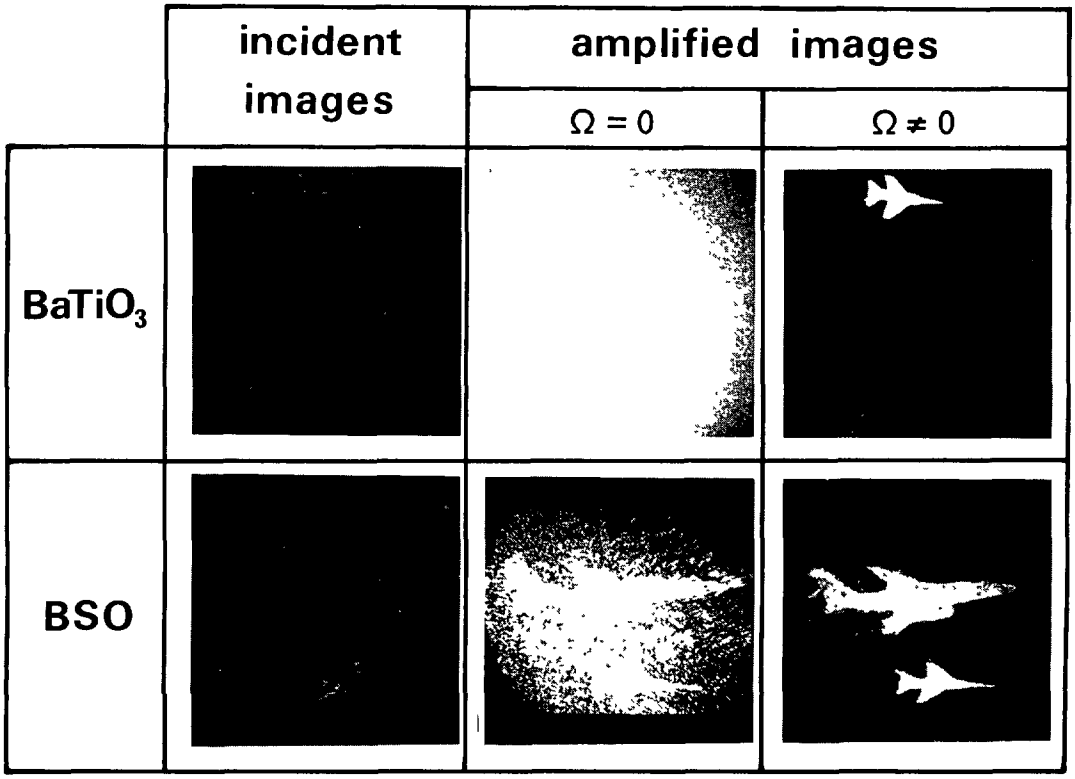

Fig. 4. — High-gain, low-noise image amplification in two-wave mixing experiments with rotating crystals. Left : low-intensity incident images. Middle : amplified images ($\times 10^3$ for $BaTiO_3$, $\times 50$ for BSO) at $\Omega = 0$; the quality of the images is corrupted by amplified scattered noise. Multiple amplified parasite images due to reflections on the crystal interfaces are also present for $BaTiO_3$. Right : noise-free amplified image ($\times 500$ for $BaTiO_3$ $\times 20$ for BSO).

3. Noise reduction by tilting a BSO crystal.

As detailed in what follows, this new noise-reduction method is most useful when the efficient interaction occurs for small angles between the injected signal and the pump beam [8]. In these crystals [e.g. BSO and GaAs] the photorefractive gain exhibits a sharp resonance effect around an optimum signal-to-pump angle. Based on the resonance in these narrow angular bandpass amplifiers, we experimentally demonstrate low-noise image amplification and picowatt wavefront detection.

The principle is based on the observation that a large contribution of the beam fanning originates from optical oscillations between the crystal faces (Fig. 5). These oscillations build-up because the exponential gain coefficient Γ is large enough to overcome the bulk absorption and interface reflection losses [9]. The conditions for these oscillations can be written as $\Gamma > \Gamma_{th}$, where

$$\Gamma_{th} = 2\left(\alpha - \frac{\mathrm{Ln}\, R}{\ell}\right)$$

Γ_{th} is the two-beam coupling threshold gain coefficient, α is the crystal absorption coefficient, R is the reflection coefficient on the crystal interface, and ℓ is the interaction length. We have

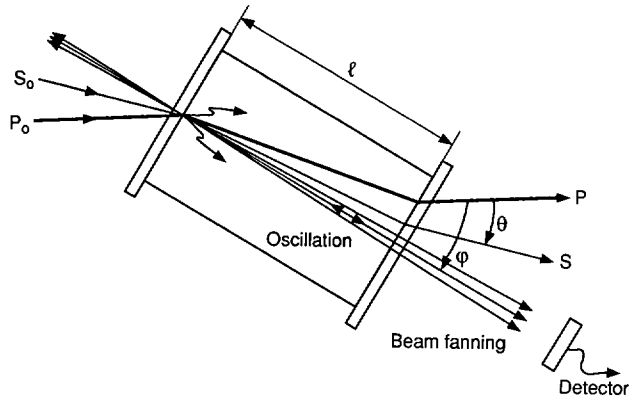

Fig. 5. — Two-wave mixing in a tilted photorefractive crystal. The optical noise is due to the Fabry-Perot oscillations between the crystal faces. The signal beam S_0 is injected in the maximum gain direction.

assumed here that energy transfer occurs only in the forward direction. Typical values for the above parameters in materials such as BSO, GaAs, and $BaTiO_3$, in their optimum gain configurations, are $\Gamma \sim 8\text{-}20\ cm^{-1}$, $\alpha \sim 1\ cm^{-1}$, $R = 0.2$, and $\ell = 1$ cm. In such conditions, the oscillation threshold is easily attained ($\Gamma_{th} \sim 5\ cm^{-1}$ with the above data), and numerous oscillation modes build up between the crystal faces. The principle of noise reduction in bandpass-type photorefractive amplifiers is shown in figure 5. The pump beam P_0 and a signal S_0 illuminate the crystal in a two-wave mixing configuration. The crystal input face is tilted by an angle φ with respect to the pump beam. Let Γ_φ be the exponential gain coefficient associated with the interaction between the pump beam and the interface oscillating modes around the angular direction φ. Then, the oscillations are not allowed to build up if $\Gamma_\varphi < \Gamma_{th}$. On the other hand, the angle θ between the pump beam and the injected signal beam is chosen for maximum two-beam coupling gain. In other words, high signal-to-noise ratios are expected when the two following conditions are met simultaneously : (i) the pump signal angle belongs to the bandwidth of the amplifier, and (ii) the oscillating noise directions are rejected out of the amplifier bandwidth.

Owing to its narrow bandpass characteristics and small optimum angle [10], BSO is used to demonstrate this new noise-reduction technique (crystal aperture 5 mm × 5 mm, interaction length 1 cm, $E_0 = 9$ kV/cm). The incident pump beam illumination is $I_{P_0} = 7.5\ mW/cm^2$ from a cw single-longitudinal-mode argon-ion laser operating at a 514.5 nm wavelength. The crystal is allowed to tilt in the horizontal and/or in the vertical directions. The total noise intensity as a function of the angular position of the crystal is shown in figure 6. The lower curves correspond to the case for which anti-reflection-coated glass plates are bound to the crystal with an index-matching oil (residual reflection ~ 7 %). The main characteristics that can be drawn from these curves are twofold. First, the optical noise intensity is lower with the antireflection glass plates on the crystal [11]. Second, the optical noise drops drastically when the crystal is strongly tilted in the horizontal (or vertical) direction. This behavior can be understood in terms of oscillating noise modes that build up between the two external crystal faces. When the crystal is tilted or antireflection coated, the number of oscillating Fabry-Perot modes that reach the threshold condition ($\Gamma_\varphi > \Gamma_{th}$) decreases, which results in an overall decrease of the optical noise in the output plane. For horizontal tilts, it is noticeable that maximum noise occurs for $\varphi = 1°$. This value is close to the optimum signal-to-pump angle $\theta \sim 1°$ that produces high gain in two-beam coupling with BSO operated in the drift mode. A 6° horizontal tilt is sufficient to suppress most of the noise at the output.

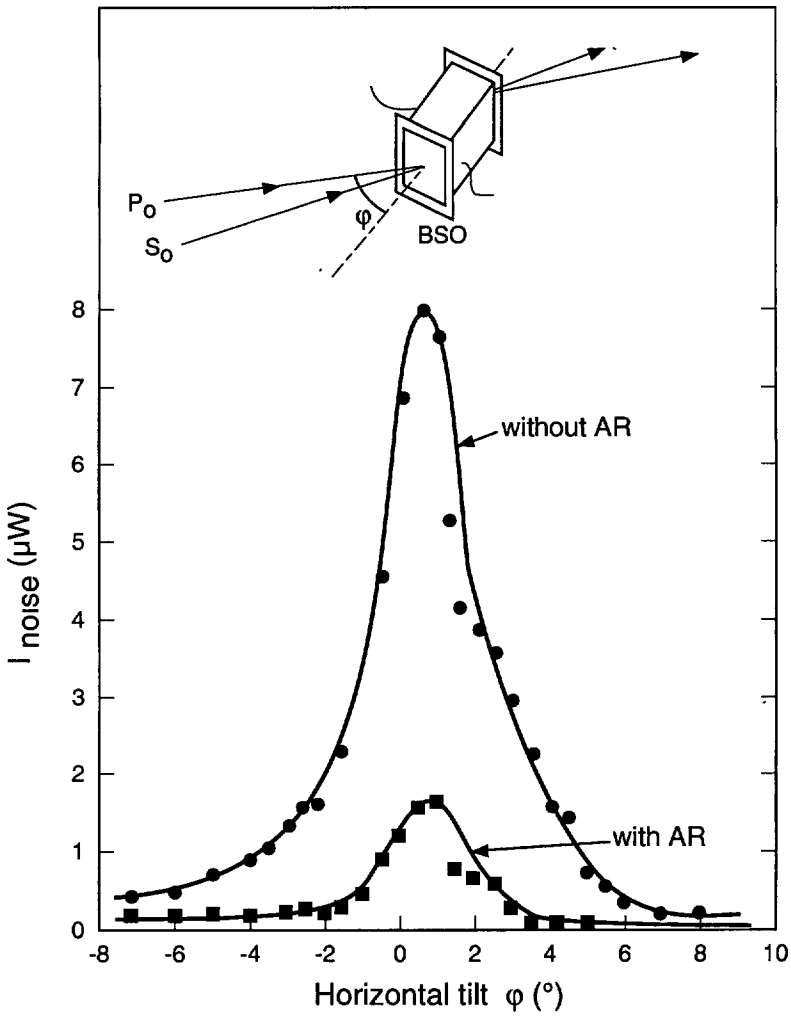

Fig. 6. — Noise power in photorefractive BSO *versus* the horizontal tilt of the crystal. AR : antireflection coated glass plate.

To demonstrate low-noise amplification of extremely weak signals carrying spatial information, we inserted a test object slide across the signal beam path in a nearly degenerate two-beam coupling configuration (moving grating recording). To improve the homogeneity across the amplified image, a diffusing screen is placed in front of the test slide. The resulting intensity at the entrance face of the crystal is $I_s = 35$ nW (Fig. 7a). The photorefractive BSO crystal is sandwiched between the two antireflection-coated glass plates and the pump-to-signal angle is adjusted for maximum coupling ($\theta = 2°$). For an untilted crystal, the amplified image is buried in a strong background noise (Fig. 7b). The crystal is then tilted in both the horizontal and vertical directions, with $\varphi = 5°$ and $\varphi' = 9{,}5°$. Figure 7c shows the amplified image. The measured input-output gain is approximately 30, and all the background noise has been removed.

The amplification of ultraweak signals is a straightforward application of this noise reduction technique. How much can we still decrease the incident beam ? This question was

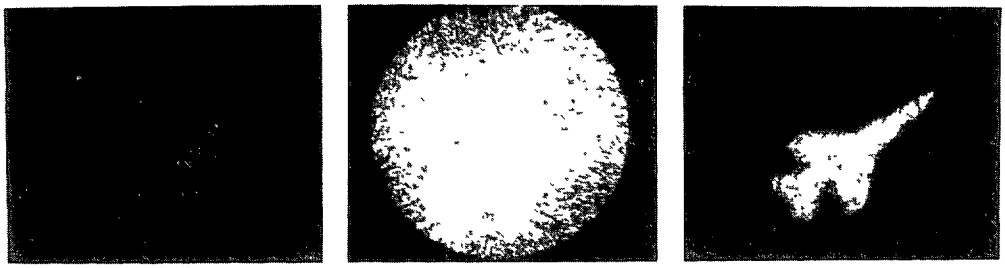

Fig. 7. — Low-noise image amplification with tilted BSO crystal : (a) input image ; (b) amplified image without tilt ($\varphi = \varphi' = 0$), $\theta = 2°$; (c) amplified image with tilt ($\varphi = 5°$, $\varphi' = 9.5°$), $\theta = 2°$.

already raised for Brillouin and Kerr nonlinear processes [12, 13]. In an attempt to provide a partial answer for photorefractives, we have further decreased the incident beam intensity by inserting neutral-density filters and hard apertures across the signal beam path. Figure 8 shows the result of such an experiment, for which the incident intensities are estimated to be 70 pW for the image and 0.5 pW for the hard-aperture-limited beam. Figures 8a and 8b show the corresponding amplified images, with measured gains of 100× and 1 000×, respectively. The lower part of figure 8b shows the partial intensity distribution around the signal and was obtained with a linear charge-coupled-detector. Considering an estimated response time of 50 ms in our experiment with BSO, we have achieved the amplification of a signal carrying approximately 10^6 photons.

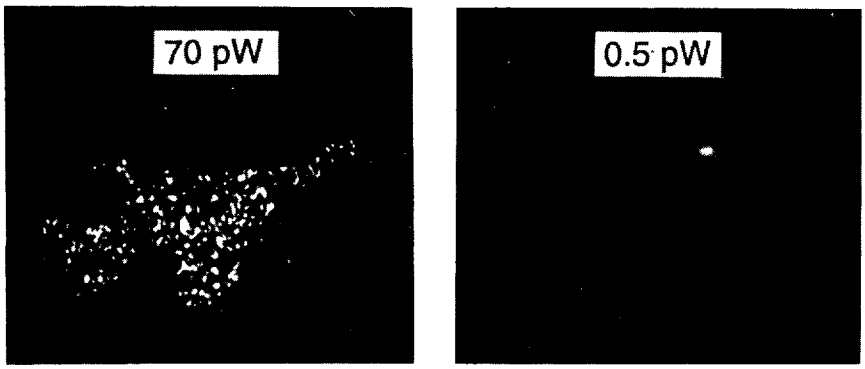

Fig. 8. — Detection of ultraweak signals : (a) 100× amplification of a 70-pW image, (b) 1 000× amplification of a 0.5-pW signal beam.

4. Application to long term readout of a photorefractive storage crystal.

We propose and experimentally demonstrate in this paragraph the realization of a long-term readout photorefractive memory by using a combination of two cascaded crystals, one for

storage and one for amplification [14]. To read out the memory, the storing crystal is illuminated with a weak-intensity beam, while the amplifying crystal operates in the high-gain low-noise configuration [8]. In this way the apparent writing-erasure cycle asymmetry is greatly improved, thus providing long-term cw readout capabilities of the storing crystal [15-17]. To demonstrate this operating principle, we have used combination of $LiNbO_3$/BSO as storage/amplifier crystals. A schematic diagram of the experiments is shown is figure 9. The storage is achieved by using an angular multiplexing technique. Three multiplexed gratings are first recorded in a 2 mm-thick, 0.015 % Fe-doped $LiNbO_3$, crystal in the following conditions : wavelength $\lambda = 514$ nm, fringe spacing $\Lambda_0 = 1$ μm, $I_R = 800$ mW/cm^2, $I_S = 150$ mW/cm^2, exposure time for each grating is $\tau \approx 20$ s, and crystal rotation between two successive recordings $\sim 0.5°$.

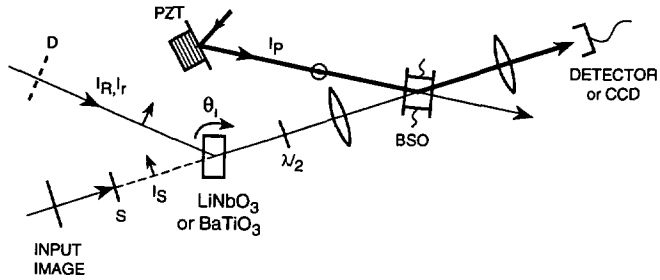

Fig. 9. — Optical layout of the experimental demonstration of long term readout memories with $LiNbO_3$/BSO and $BaTiO_3$/BSO combinations as storing/amplifying crystals. D, neutral-density filter (used in the readout step only) ; $\lambda/2$ half-wave plate ; PZT, piezoelectric transducer.

The lower curve in figure 10 shows a readout experiment at high-level intensity $I_R = 40$ mW/cm^2. Here the output-beam intensity is measured as function of time. The initial diffraction efficiency is 8 %. In these conditions, the complete decay of the recorded gratings takes approximately 150 min. In a second experiment, the three gratings are recorded again in the same conditions, but now the $LiNbO_3$ crystals is read out at a much lower level $I_r = 0.83$ mW/cm^2. To compensate for this reduction, the diffracted beam undergoes low noise amplification in the BSO and it now results a memory time in $LiNbO_3$ of more than 24 h. In figure 11, the two beam coupling in the tilted BSO amplifies the extremely weak diffracted image from the $LiNbO_3$ crystal. The gain factor is controlled by the electric field applied to the BSO crystal and it is adjusted so that the decrease due to low intensity reading of the $LiNbO_3$ is recovered by the amplification process. In such conditions, the $LiNbO_3$ memory can be used for more than 20 h without significant decay of the output intensity.

5. Conclusions.

We have reviewed in this paper new methods allowing high gain and low noise image amplification in a photorefractive crystal. As an example, the amplification of 70 pW intensity images has been demonstrated as well as the detection of subpicowatt signal after amplification through two-wave mixing in a tilted BSO crystal. Starting from these established results it now appears important to investigate both from the theory and the experiments, which is the lowest usable signal beam intensity which can be amplified by the nonlinear crystal. Reaching this limit it is expected that photon noise limited photorefractive amplifiers can be realized for the coherent detection of complex wavefronts carrying spatial and temporal informations. These

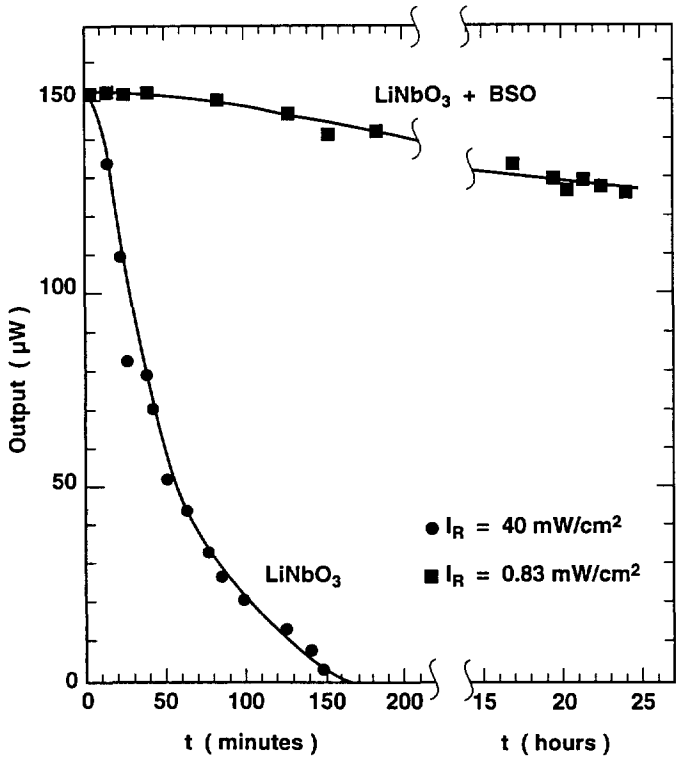

Fig. 10. — Memory output as a function of time for the $LiNbO_3$/BSO combination. Lower curve, high-intensity readout beam in $LiNbO_3$ and no amplification in BSO ; upper curve, low-intensity readout with amplification in BSO.

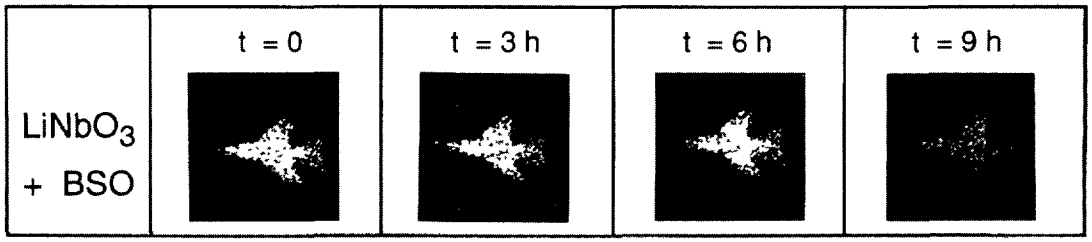

Fig. 11. — Memory output at different time intervals for $LiNbO_3$/BSO. The storing crystals ($LiNbO_3$) is continuously illuminated with intensities of 2 mW/cm^2.

concepts are also quite attractive for implementing optical architectures where the information of an image should be transfered in parallel to optical storage and processing units.

Acknowledgements.

The authors gratefully acknowledge A. Delboulbé and S. Bann for their very helpful contribution to this work.

References

[1] KUKHTAREV N. V., MARKOV V. B., ODULOV S. G., SOSKIN M. J. and VINETSKII V. L., *Ferroelectrics* **22** (1979) 949.

[2] Photorefractive materials and their applications, Topics in Applied Physics, P. Günter, J.-P. Huignard, Eds., vol. **61-62** (Springer Verlag, Berlin, 1989).

[3] YEH P., *IEEE J. QE* **25** (1989) 484.

[4] VALLEY G. C. and KLEIN M. B., *Opt. Eng.* **22** (1983) 704.

[5] FEINBERG J., *J Opt. Soc. Am.* **72** (1982) 46.

[6] RAJBENBACH H., DELBOULBÉ A. and HUIGNARD J.-P., *Opt. Lett.* **14** (1989) 1275.

[7] Amplified scattered noise can also be exploited to implement temporal high-pass filters as reported in :
CRONIN-GOLOMB M., BIERNACKI A. M., LIN C. and KONG H., *Opt. Lett* **12** (1987) 1029 ;
FORD J. E., FAINMAN Y. and LEE S. H., *Opt. Lett.* **13** (1988) 856.

[8] RAJBENBACH H., DELBOULBÉ A. and HUIGNARD J.-P., *Opt. Lett.* **16** (1981) 1481.

[9] ODULOV S. G. and SOSKIN M. S., In Photorefractive Materials and Their Applications II, Survey of Applications, P. Günter and J.-P. Huignard Eds. (Springer-Verlag, Berlin, 1989), pp. 27-33, and references therein.

[10] RAJBENBACH H., HUIGNARD J.-P. and LOISEAUX B., *Opt. Comm.* **48** (1983) 247.

[11] KARIM Z., GARRET M. H. and TANGUAY A. R. Jr., in Digest of Optical Society of America Annual Meeting (Optical Society of America, Washington, D.C. 1988) paper WA. A7.

[12] ANDREEV N. F., BESPALOV V. I., DVORETSKY M. A. and PASMANIK G. A., *IEEE J. Quantum Electron.* **25** (1989) 346.

[13] MCGRAW R., ROGOVIN D. and GAVRIELIDES A., *Appl. Phys. Lett.* **54** (1989) 199.

[14] RAJBENBACH H., BANN S. and HUIGNARD J.-P., *Opt. Lett.* **17** (1992) 1712.

[15] SASAKI H., FAINMAN Y., FORD J. E., TAKETOMI Y. and LEE S. H., *Opt. Lett.* **16** (1991) 1874.

[16] BOJ S., PAULIAT G. and ROOSEN G., *Opt. Lett.* **17** (1992) 438.

[17] MANILOFF E. S. and JOHNSON K., *J. Appl. Phys.* **70** (1991) 4702.